HHS Public Access

Author manuscript

Hypertens Res. Author manuscript; available in PMC 2021 November 13.

Published in final edited form as:

Hypertens Res. 2021 August ; 44(8): 906–917. doi:10.1038/s41440-021-00661-x.

Increased AT_1 Receptor Expression and Its Mediated Vasoconstriction Lead to Hypertension in *Snx1*$^{-/-}$ Mice

Chao Liu[1,2,#], **Xingyue Li**[5,6,1,#], **Jinjuan Fu**[1,2], **Ken Chen**[1,2], **Qiao Liao**[1,2], **Jialiang Wang**[1,2], **Caiyu Chen**[1,2], **Hao Luo**[1,2], **Pedro A. Jose**[3], **Yongjian Yang**[5,6,*], **Jian Yang**[4,*], **Chunyu Zeng**[1,2,7,8,*]

[1]Department of Cardiology, Daping Hospital, Army Military Medical University, Chongqing, China

[2]Chongqing Institute of Cardiology & Chongqing Key Laboratory of Hypertension Research, Chongqing, China

[3]Division of Renal Disease & Hypertension, The George Washington University School of Medicine and Health Sciences, Washington, DC, United States

[4]Department of Clinical Nutrition, The Third Affiliated Hospital of Chongqing Medical University, Chongqing, China

[5]College of Medicine, Southwest Jiaotong University, Chengdu, Sichuan, China

[6]Department of Cardiovascular Medicine, The General Hospital of Western Theater Command PLA, Chengdu, Sichuan, China

[7]State Key Laboratory of Trauma, Burns and Combined Injury, Daping Hospital, The Third Military Medical University, Chongqing, P.R. China.

[8]Cardiovascular Research Center of Chongqing College, Department of Cardiology of Chongqing General Hospital, University of Chinese Academy of Sciences, Chongqing, P.R. China.

Abstract

Angiotensin II type 1 receptor (AT_1R) is a vital therapeutic target for hypertension. Sorting nexin 1 (SNX1) participates in the sorting and trafficking of renal dopamine D_5 receptor, while angiotensin and dopamine are counter-regulatory factors in regulating blood pressure. Thus, we supposed whether SNX1 has an effect on the AT_1R sorting and trafficking. *Snx1*$^{-/-}$ mice, generated using the CRISPR/Cas9 system, showed a dramatic elevation in blood pressure compared to wild-type littermates. The angiotensin II-mediated contractile reactivity of mesenteric arteries and AT_1R expression in aortas also rised in *Snx1*$^{-/-}$ mice. Moreover, immunofluorescence and immunoprecipitation analysis, respectively, revealed that SNX1 and AT_1R were colocalized and interacted in aortas from wild-type mice. *In vitro* studies disclosed that AT_1R protein level and its downstream calcium signaling were upregulated in A10 cells treated with SNX1 siRNA. This may result from decreased AT_1R protein degradation because AT_1R mRNA level had no change,

[*]**Corresponding authors:** Jian Yang, jianyang@hospital.cqmu.edu.cn, Chunyu Zeng, chunyuzeng01@163.com, Yongjian Yang, yyj10001@126.com.

[#]These authors contributed equally.

Conflict of Interest

The authors declare that they have no conflict of interest.

but the expression of AT_1R protein was less degraded when SNX1 knockdown, as reflected by the cycloheximide chase assay. Furthermore, the proteasomal rather than lysosomal inhibition increased AT_1R protein content, accompanied by decayed binding of ubiquitin and AT_1R after SNX1 knockdown. Confocal microscopy uncovered that AT_1R colocalized with PSMD6, a proteasome marker, and the colocalization was reduced after SNX1 knockdown. These findings suggest that SNX1 sorts AT_1R to proteasomal degradation and SNX1 impairment increases arterial AT_1R expression, leading to higher vasoconstriction and increased blood pressure.

Keywords

Sorting nexins; Angiotensin II type 1 receptor; Vascular smooth muscle; Blood pressure

Introduction

Hypertension, one of the most common chronic diseases worldwide, has been identified as the leading risk factor for cardiovascular events such as heart attack, heart failure, aneurysm, chronic kidney disease, stroke, cognitive impairment, and dementia [1]. Despite substantial progress has been made in understanding the epidemiology, pathophysiology, and risk associated with hypertension, hypertension and its complications remain a heavy burden of global medical care [2, 3].

Pathophysiological changes of the vasculature have been considered to play a critical role in the development of hypertension [4-6]. Blood vessels are not merely mechanical channels through which the blood flows, a variety of receptors distributed there, exerting their physiological functions in modulating blood pressure. Angiotensin II (Ang II), a crucial effector hormone, causes vasoconstriction and blood pressure increment, while Ang II type 1 receptor (AT_1R), a G protein-coupled receptor (GPCR) mediating most effects of Ang II, is well known to participate in the process of hypertension. Both AT_1R expression and functions are enhanced in hypertension [7, 8]. Furthermore, AT_1R is not only involved in the contraction of vascular smooth muscle cells (VSMCs) [9], but also related to other pathophysiological alterations such as increased oxidative stress [10, 11], chronic inflammation [12, 13] and cardiovascular remodeling [14, 15].

The balance of GPCR recycling and degradation is pivotal for cellular homeostasis, while the perturbation of it may lead to impaired homeostatic responses and morbid states such as coronary artery disease and hypertension [16-18]. Sorting nexins (SNXs), a diverse group of cellular sorting proteins characterized by the phox homology (PX) domain that can bind to phosphoinositide [19], are key in orchestrating the process of protein sorting and trafficking including endocytosis, endosomal sorting, and endosomal signaling [16]. Studies in human renal proximal tubule cells (hRPTCs) and in mice have shown that SNXs exert their physiological effects via regulating the expression and function of GPCRs [20-22], and SNXs impairment-caused GPCR dysfunction is associated with cardiovascular diseases [16, 23]. Among SNXs, SNX1 is the first mammalian sorting nexin that characterized and is the ortholog of the yeast vacuolar protein-sorting (Vps)5p, a protein involved in trans-Golgi network trafficking [24]. Previous studies have reported that renal SNX1 is involved in blood

pressure modulation via sorting and recycling the dopamine D_5 receptor (D_5R) back to the cell membrane in hRPTCs [20]. However, whether arterial SNX1 exerts physiological effects in blood pressure regulation is still unknown. Moreover, Ang II and dopamine are counter-regulatory hormones participating in blood pressure controlling [25, 26]. Thus, we speculated that arterial SNX1 may take part in the sorting and trafficking of AT_1R in vascular smooth muscle cells (VSMCs). The aim of this present study was to investigate the regulation of SNX1 on the expression and function of arterial AT_1R and its underlying mechanisms.

Methods

Transgenic mice

The SNX1-deficient mice in C57BL/6 background were generated via CRISPR/Cas9-mediated genome engineering by Cyagen (Cyagen Biosciences, Guangzhou, China). The mouse SNX1 gene (GenBank accession number: NM_019727.2) is located on mouse chromosome 9, and the exon 1 was selected as the target site. Cas9 mRNA and guide RNAs (gRNAs) (gRNA1: 5'-CCCTGGCATGGATCCGGAGTCGG-3'; gRNA2: 5'-GGATATTTTCACTGGCGCCGCGG-3') generated by *in vitro* transcription were injected into fertilized eggs for knockout mouse productions. The founders were genotyped by polymerase chain reaction (PCR) followed by DNA sequencing analysis. Then the positive founders were breeding to the next generation which was genotyped by PCR and agarose gel electrophoresis.

Genotyping of *Snx1*$^{-/-}$ mice

Genomic DNA was extracted from mouse tail tissue using mammalian genomic DNA extraction kit (Beyotime, Jiangsu, China). The target DNA was amplified by PCR using the specific primers (forward: 5'-CAGCCTTGCGGTTCAGTGCTT-3'; reverse: 5'-AAATGCCCGCTGAATCCTTGG-3'), and the PCR was carried out in the following conditions: 1 μL of template at a concentration of 100 ng/μL, 10 μL of GoTaq Green Master Mix (Promega, Madison, WI, USA), 1 μL forward primer (10 μmol/L, Sangon Biotech, Shanghai, China), 1 μL reverse primer (10 μmol/L, Sangon Biotech, Shanghai, China), and nuclease-free water (Promega, Madison, WI, USA) was added to a final volume of 20 μL per reaction.

The PCR protocol consisted of an initial denaturing step at 95 °C for 3 min, 30 cycles at 95 °C for 30 s, 59 °C for 30 s, and 72 °C for 1 min, followed by a final extension at 72 °C for 5 min in a T100™ thermal cycler (Bio-Rad, Hemel Hempstead, UK). Then the PCR products were then analyzed by 1% agarose gel electrophoresis.

Measurement of blood pressure

Blood pressure of mice was measured by the tail-cuff plethysmography method using a programmed electro-sphygmomanometer Softron BP-2010A (Softron Biotechnology, Beijing, China) as described previously [27-29]. Briefly, 10-week-old mice were trained to adapt to the environment before blood pressure measurement. The mice were gently placed in a small soft cage without being anesthetized, and after a period time of stabilization

of their behavior and heart rates, the systolic, diastolic and mean blood pressures were recorded, and the average of 10 recorded values was used for further statistical analysis.

Preparation and study of small resistance arteries

Mesenteric artery ring studies were performed according to previous reports [30-32]. In brief, second-order mesenteric artery branches were cut into 2 mm rings, and then each segment was suspended between two tungsten wires (25 μm in diameter) in chambers of a Multi Myograph System (DMT-620, Aarhus, Denmark) to measure isometric tension, and the chambers were filled with physiological saline solution (PSS) and continuously bubbled with carbogen (95% O_2, 5% CO_2) at 37 °C [33]. After a 15-min equilibration period, mesenteric arterial rings were stretched to the optimal luminal diameter for active tension development. In the first set of experiments, rings were contracted with phenylephrine HCl (PHE; 10 μmol/L) and high-potassium PSS (125 mmol/L) to reach the maximum tension, followed by rinse with PSS. Then different drugs were administrated to test the reactivity of artery rings, and the response curves were measured by a cumulative concentration-dependent protocol.

Immunohistochemical and immunofluorescent staining of the aortas

Aorta samples were fixed in 4% paraformaldehyde and dehydrated in increasing concentrations of ethanol. Samples were then cleared in xylene and embedded in paraffin. The samples were cut into 4 μm thick sections for further experiments. The immunohistochemical staining was carried out using a rabbit anti-AT_1R antibody (1:100, Proteintech, Wuhan, China). Reactions were detected by horseradish peroxidase-conjugated goat anti-rabbit IgG and the color was developed with 3,3'-diaminobenzidine tetrahydrochloride (Solarbio, Beijing, China) and stopped by rinsing in deionized water.

For the immunofluorescent staining of aortic sections, we followed the protocol described previously [34]. In brief, the sections were permeabilized and blocked, then primary antibodies (rabbit anti-AT_1R, 1:100, Proteintech, Wuhan, China; goat anit-SNX1, 1:100, Sigma-Aldrich, St. Louis, MO, USA) were incubated overnight at 4 °C. After rinse, the secondary antibodies (Alexa Fluor 488-labeled goat anti-rabbit IgG 1:100, Zsbio, Beijing, China; Cy3-conjugated affinipure donkey anti-goat IgG 1:100, Proteintech, Wuhan, China) were applied for 1 h at room temperature, while for negative controls, the samples were incubated with the isotypematched control primary antibodies. Additionally, the 4',6-diamidino-2-phenylindole (DAPI) was used to stain nuclei. Colocalization analysis was performed with the ImageJ Colocalization Finder plugin, and the Pearson's correlation coefficient (Rr) and the overlap coefficient (R) were calculated [35-37].

Cell culture

Embryonic thoracic aortic smooth muscle cells (passage 10~20) from normotensive Berlin-Druckrey IX rats (A10; CRL 1476, ATCC) were cultured at 37 °C in 95% air and 5% CO_2 in Dulbecco's modified Eagle's medium (DMEM, HyClone, South Logan, UT, USA) supplemented with 10% v/v fetal bovine serum (Invitrogen Life Technologies, Karlsruhe, Germany) and 1% v/v penicillin/streptomycin (Invitrogen Life Technologies, Karlsruhe, Germany).

SNX1 knockdown via small interfering RNA

The small interfering RNA (siRNA) against SNX1 mRNA and its control scrambled siRNA were purchased from Ruibo Biotechnology (Guangzhou, China). The target sequence of *Snx1* siRNA (siSNX1) was 5'-GCCTAATAGGAATGACAAA-3', the sense strand was 5'-GCCUAAUAGGAAUGACAAAdTdT-3', and the antisense strand was 5'-UUUGUCAUUCCUAUUAGGCdTdT-3'. The RNA interference experiments were performed using Lipofectamine RNAiMAX Reagent (Invitrogen, Carlsbad, CA, USA) according to the manufacturer's instruction. Briefly, cells were cultured in 6-well plates until 60% confluence, then 30 pmol siSNX1, scrambled siRNA and negative control were mixed with 9 μL of RNAiMAX, respectively, in 150 μL of Opti-MEM (Invitrogen, Carlsbad, CA, USA). Cells were then incubated for 24 h for mRNA extraction or 48 h for protein extraction.

Immunoblotting

Immunoblotting studies were performed according to procedures described in our previous reports [38, 39]. Briefly, proteins were extracted from mice aortas or A10 cells with ice-cold Tissue Extraction Reagent (Thermo Scientific, Waltham, MA, USA) containing protease inhibitor cocktail (Roche, Indianapolis, IN, USA). Protein samples (50 μg) were separated by 10% sodium dodecyl sulfate polyacrylamide gel electrophoresis, followed by electron-transferring to nitrocellulose membranes. Ponceau S staining was used as quality control for the transferring. Then, the blocked membranes were incubated at 4°C overnight with primary antibodies including rabbit anti-AT_1R antibody (1:500, Proteintech, Wuhan, China), rabbit anti-AT_2R antibody (1:300, Beyotime, Jiangsu, China), rabbit anti-D_5R antibody (1:500, Proteintech, Wuhan, China), rabbit anti-SNX1 antibody (1:1000, Thermo Fisher Scientific, Waltham, MA, USA), and mouse anti-GAPDH (1:5000, Proteintech, Wuhan, China). The blotted membranes were then washed and incubated with the IRDye 800 labeled goat anti-rabbit secondary antibody (1:15000, Li-Cor Biosciences, NE, USA) or IRDye 680 labeled goat anti-mouse secondary antibody (1:15000, Li-Cor Biosciences, NE, USA) at room temperature for 1 h. Membranes were washed 3 times in Tris-buffered saline/Tween (TBST), and bands were detected using the Odyssey Infrared Imaging System (Li-Cor Biosciences, NE, USA). The images were analyzed using the ImageJ Software to obtain integrated intensities.

Enzyme-linked immunosorbent assay

The supernatants of cultured A10 cells were collected and centrifuged at 1000 × g at 4 °C for 20 min, then the levels of Ang II were assessed by the enzyme-linked immunosorbent assay (ELISA) kit (Cloud-Clone Corp., Wuhan, China) according to the manufacture's instruction. The absorbance was measured at 450 nm, and the concentration of Ang II was calibrated with the standard curve.

Real-time quantitative polymerase chain reaction

SNX1 and AT_1R mRNA levels in mice aortas or A10 cells were quantified by real-time quantitative polymerase chain reaction (qPCR) with forward and reverse primers (Table 1), following the protocol in our previous study [38]. The following PCR condition was applied:

95°C for 3 min, 40 cycles at 95°C for 10 sec and 62°C for 30 sec followed by 62°C 10 sec. Since there are several different transcriptional variants of mouse GAPDH, mouse β-actin was used instead as the internal control.

Immunoprecipitation

Equal amounts of cell lysates (1000 μg total protein) were incubated with anti-SNX1 antibody (5 μg; SNX1-AT_1R immunoprecipitation) or anti-ubiquitin antibody (5 μg, Proteintech, Wuhan, China) overnight at 4°C, then 50 μL protein G Plus-agarose beads (Santa Cruz, CA, USA) were added and incubated for another 4 h at 4°C. The immunoprecipitates were subjected to immunoblotting with anti-AT_1R antibody. Additionally, rabbit IgG (negative control) and AT_1R antibody (positive control) were used as the immunoprecipitants to test the specificity of the bands on the immunoblots.

Confocal microscopy

A10 cells (1×10^4 cells/well) were seeded in the 20 mm Glass Bottom Culture Dishes (Nest, Wuxi, China). After incubated with siSNX1 for 48 h, cells were fixed with 4% paraformaldehyde for 30 minutes at 4°C, followed by permeabilization and blocking with the Immunostaining Blocking Buffer (Sangon Biotech, Shanghai, China). The cells were then incubated overnight at 4°C with primary antibodies including mouse anti-AT_1R antibody (1:50, Santa Cruz, CA, USA), rabbit anti-SNX1 antibody (1:100, Thermo Fisher Scientific, Waltham, MA, USA), rabbit anti-PSMD6 antibody (1:100, Sigma-Aldrich, St. Louis, MO, USA) and rabbit anti-LAMP1 antibody (1:100, Sigma-Aldrich, St. Louis, MO, USA). For checking the colocalization of AT_1R and Rab5, the rabbit anti-AT_1R antibody (1:100, Proteintech, Wuhan, China) and mouse anti-Rab5 (1:50, Santa Cruz, CA, USA) were applied. After incubation with the secondary antibody (Alexa Fluor 488-labeled goat anti-rabbit IgG 1:100, Zsbio, Beijing, China; Cy3-conjugated affinipure goat anti-mouse IgG, 1:100, Proteintech, Wuhan, China) and DAPI, samples were observed under confocal microscope (Olympus Corporation, Tokyo, Japan). Colocalization analysis was performed with the ImageJ Colocalization Finder plugin. The index of colocalization corresponds to the mean ± standard deviation (SD) of the overlap coefficient (R)×100 obtained for at least 10 cells for each colabeling [37].

Intracellular calcium measurement

Intracellular calcium was labeled by Fluo-4 AM (Beyotime, Jiangsu, China) following the manufacturer's instruction. Briefly, cells were plated in 6-well plates, loaded with 5 μM Fluo-4AM for 30 min at 37 °C, and then incubated in the dark for another 30 min. Cells were treated with Ang II (10^{-7} mol/L) with or without 15 minutes of losartan (10^{-5} mol/L) pretreatment [7]. Images were captured and analyzed as described previously [40, 41], and quantifications were performed using the ImageJ software.

Statistical analysis

Data were expressed as mean ± SD values. Statistical significance was tested via ANOVA followed by a post hoc Dunnett's test for multi-group (>2) comparison, and Student's t-test was used for two-group comparison. For assays involving mesenteric arterial rings, the

comparison was made by repeated-measures ANOVA (or paired t-test when only 2 groups were compared) [32]. A value of $P<0.05$ was considered statistically significant.

Results

Generation and identification of the *Snx1*$^{-/-}$ mice

The *Snx1*$^{-/-}$ mice in C57BL/6 background were generated using CRISPR/Cas9-mediated genome engineering, as the schematic diagram illustrated (Fig. 1a). The offsprings were genotyped by PCR and agarose gel electrophoresis, the homozygous genotype (*Snx1*$^{-/-}$) showed a single band of 565 base pairs (bp), the wild-type (WT, *Snx1*$^{+/+}$) showed a single band of 645 bp, and the heterozygous genotype (*Snx1*$^{+/-}$) showed both bands of 565 and 645 bps (Fig. 1b). Furthermore, the qPCR and immunoblotting results, respectively, showed that there were SNX1 mRNA and protein expressions in aortas from WT mice, but not from *Snx1*$^{-/-}$ mice (Fig. 1c, d).

Elevated blood pressure and enhanced reactivity of mesenteric artery to Ang II in *Snx1*$^{-/-}$ mice

The *Snx1*$^{-/-}$ mice showed elevated systolic blood pressure (Fig. 2a), diastolic blood pressure (Fig. 2b) and mean blood pressure (Fig. 2c) compared to their WT littermates, as measured by the tail-cuff method. The artery ring studies indicated that there were no obvious differences between *Snx1*$^{-/-}$ and WT mice in PHE-induced contraction (Fig. 3a) and SNP-mediated relaxation (Fig. 3b). However, the Ang II-induced contraction was the most remarkably changed among the applied drugs, in which the Ang II-induced contraction of mesenteric arteries was much higher in *Snx1*$^{-/-}$ mice than WT littermates (Fig. 3c).

Increased AT_1R expression in aortas from *Snx1*$^{-/-}$ mice

We next investigated the expression of main receptors of Ang II, and found that AT_1R protein level was significantly elevated in aortas from *Snx1*$^{-/-}$ mice, as reflected by the immunoblotting result (Fig. 4a). Similarly, immunohistochemical staining of AT_1R also suggested increased AT_1R expression in aortas from *Snx1*$^{-/-}$ mice compared to WT littermates (Fig. 4b). However, the expression of AT_2R, another Ang II receptor, was not different between *Snx1*$^{-/-}$ and WT mice (Fig. 4c). Besides, the expression of D_5R, another GPCR that has been shown to promote AT_1R degradation [42], was not changed in aortas from *Snx1*$^{-/-}$ mice (Fig. 4d). Furthermore, we tested if there was interaction between SNX1 and AT_1R in aortas from WT mice via the immunofluorescence laser confocal microscopy, the results of the quantification indicated that SNX1 and AT_1R were colocalized in tunica media (Fig. 4e). The results of immunoprecipitation also suggested that SNX1 could bind to AT_1R in the aortas (Fig. 4f).

Upregulated AT_1R protein level in SNX1 knockdown A10 cells

In vitro studies in A10 cells also confirmed that the protein expression of AT_1R was upregulated after SNX1 knockdown via specific siRNA (Fig. 5a). Moreover, the calcium signal, which could be activated by the stimulation of AT_1R and then causes VSMC contraction [9, 43], was elevated in siSNX1-treated A10 cells in the basal state and increased more significantly after Ang II treatment. However, when pretreated with losartan, an AT_1R

antagonist, the elevation in calcium concentration was abolished (Fig. 5b). Furthermore, we checked the colocalization between Rab5, an endosome marker, and AT_1R after SNX1 knockdown. The quantified results from confocal microscopy disclosed an increase in AT_1R mean fluorescence intensity but a decrease in the colocalization of Rab5 and AT_1R in siSNX1-treated A10 cells (Fig. 5c). Additionally, we tested the content of Ang II, the ligand of AT_1R, in supernatants, and found that it was not altered after SNX1 knockdown (Fig. 5d). Moreover, the immunoprecipitation indicated the interaction between AT_1R and SNX1 in A10 cells (Fig. 5e).

Involvement of the proteasome pathway in SNX1-mediated AT_1R protein degradation

We further explored the underlying mechanism by which AT_1R protein level rised. The qPCR was performed and its result showed that the AT_1R mRNA level was not changed when SNX1 knockdown (Fig. 6a). However, AT_1R protein was less degraded in siSNX1-treated A10 cells at different time points in the presence of cycloheximide (500 μmol/L) [44] which inhibited *de novo* protein synthesis (Fig. 6b). This indicated that upregulated AT_1R protein level was result from reduced degradation, rather than increased mRNA expression. We further added chloroquine (100 μmol/L) [45] or clasto-lactacystin beta-lactone (CLBL, 10 μmol/L) [46], respectively, to inhibit the activity of lysosomes or proteasomes, and found no change of AT_1R content after chloroquine and cycloheximide co-treatment, but it was markedly increased after CLBL and cycloheximide co-treatment, and the difference was more pronounced in siSNX1-treated A10 cells. (Fig. 6c). Additionally, the immunoprecipitation showed that there was an interaction between ubiquitin and AT_1R, which was decreased after SNX1 knockdown (Fig. 6d). Moreover, the results of immunofluorescence laser confocal microscopy revealed that AT_1R mainly colocalized with PSMD6, a proteasomal marker, rather than LAMP1, a lysosomal marker, at the cytoplasm of A10 cells, and the colocalization of AT_1R and PSMD6 was reduced after SNX1 knockdown (Fig. 6e).

DISCUSSION

The present study suggests that SNX1 plays an important role in the regulation of arterial AT_1R expression and function; deficiency of SNX1 in mice leads to increased AT_1R protein expression and enhanced AT_1R protein function in arteries. Mechanistically, SNX1 interacts with AT_1R and participates in AT_1R sorting and trafficking to the proteasome for its degradation in A10 cells. Thus, SNX1 is involved in the regulation of blood pressure.

SNX1 is originally identified as a sorting protein interacts with the cytoplasmic sequences, including the tyrosine kinase domain and the adjacent lysosomal targeting signal, of the epidermal growth factor receptor (EGFR), and vital in the degradation of EGFR [47, 48]. More importantly, in hRPTCs, SNX1 initiates the sorting of ligand-activated D_5R at the plasma membrane by tagging the receptor for endocytosis, which has a crucial effect on D_5R trafficking; further studies in mice have found that renal specific SNX1 depletion via the renal subcapsular infusion of siSNX1 resulted in blunted natriuretic response to D_5R stimulation and elevated blood pressure [20]. Our present study shows that compared with WT littermates, the systolic blood pressure, diastolic blood pressure and mean blood

pressure of *Snx1*$^{-/-}$ mice were all elevated. It is a limitation that the blood pressure was measured by the noninvasive tail-cuff method. However, the result was consistent with our previous study, in which the blood pressure was accessed by telemetry [49], a more accurate and reliable but invasive technique [50]. These studies all suggest that SNX1 plays a vital role in the regulation of blood pressure. However, our previous study only disclosed increased renal oxidative stress and impaired natriuretic in the kidney in *Snx1*$^{-/-}$ mice [49], but not investigated the role of SNX1 in the regulation of blood vessels, which also contribute to hypertension. Thus, in our present study, we explored the effects of SNX1 on the vascular tone and its intrinsic mechanisms.

There are multiple humoral systems related to high blood pressure, among which the renin-angiotensin system (RAS) has attracted the most attention. Ang II is classically considered as the main mediator of RAS and exerts its effects via two major distinct GPCRs: the AT_1R and the AT_2R. Most Ang II actions are mediated by AT_1R, which is involved in the development of hypertension via increasing vasoconstriction [9, 51], renal sodium reabsorption [52], inducing vasopressin release [53], and facilitation of sympathetic nerve activity [54]. Thus, the regulation of AT_1R expression and function is of great significance for the prevention and treatment of hypertension. However, little attention has been paid to the sorting and trafficking of AT_1R and its effect on blood pressure. Our current study focused on the pivotal role of SNX1 in AT_1R sorting and explored the underlying mechanisms, which might indicate a novel aspect of blood pressure regulation. Our studies in small resistance arteries revealed that, among the applied drugs, Ang II-induced contraction was much enhanced in *Snx1*$^{-/-}$ mice. This might be ascribed to upregulated AT_1R expression, because AT_1R protein level was increased in both aortas from *Snx1*$^{-/-}$ mice and SNX1 knockdown A10 cells. Similar results were found in previous studies which show elevated AT_1R expression in siSNX1 treated mice kidneys [20], kidneys from *Snx1*$^{-/-}$ mice [49] and siSNX1 transfected hRPTCs [20]. Furthermore, to evaluate the function of AT_1R in siSNX1 treated A10 cells, we tested the concentration of intracellular calcium, which could be activated by stimulation of AT_1R and then causes VSMC contraction [55, 56], as did in our previous investigation [7]. We found it was significantly elevated in siSNX1-treated A10 cells in the basal state, and the difference was more pronounced after Ang II treatment. More importantly, the elevation could be blocked by pretreatment of losartan, an inhibitor of AT_1R. These results uncovered a crucial role of SNX1 in the regulation of AT_1R expression and function in VSMCs, and SNX1 depletion could lead to increased AT_1R protein level and higher Ang II-mediated mesenteric artery contractility, which further contributes to hypertension. However, one limitation of our present study is the lack of losartan-blocking experiments *in vivo* or *ex vivo*, which needs to be improved in future studies.

We next investigated regulatory mechanisms of SNX1 on AT_1R expression, and found that AT_1R protein but not mRNA level was elevated after SNX1 knockdown in A10 cells, suggesting SNX1 may be involved in the process of AT_1R protein degradation. The cycloheximide chase assay, a classical method to analyze protein degradation [57, 58], further revealed that AT_1R protein expression was increased in siSNX1-treated A10 cells after incubation with cycloheximide [44], proving the reduced AT_1R protein degradation after SNX1 knockdown. Moreover, immunofluorescence laser confocal microscopy and

immunoprecipitation assay, respectively, indicated the spatial colocalization and physical interaction in aortas and A10 cells. Since colocalization has been often conducted in a rather ad hoc fashion, and could be subject to misinterpretation and inconsistencies [59-61], we quantified the colocalization via ImageJ as previous reports [35-37]. It should be noted that the Forster resonance energy transfer (FRET) and proximity ligation assay (PLA) are more reliable methods to investigate the protein-protein interactions, to which more attention should be paid in future investigations. *In vitro* studies also showed that the colocalization of AT_1R and Rab5 was reduced in siSNX1-treated A10 cells, which indicated the role of SNX1 in AT_1R sorting. SNX1 has also been found to modulate functions of renal D5R, which mediates renal tubular AT_1R degradation [20, 42]. Thus, we further explored the expression of aortic D_5R in *Snx1*$^{-/-}$ mice, but found no obvious change. Therefore, we proposed that the regulation of aortic AT_1R by SNX1 might be independent of D_5R.

The proteasomes and lysosomes represent two most important proteolytic machineries in cells [62, 63]. The activity of GPCRs could be tightly controlled by their endocytosis, which drives the receptors into divergent lysosomal and recycling pathways [64], while the signaling proteins may also undergo regulated ubiquitination in response to GPCR activation, and the regulated ubiquitination could cause proteasomal degradation [65]. AT_1R has been reported to be degraded through the ubiquitin-proteasome pathway mediated by activation of D5R in hRPTCs [42]. This is also confirmed by another study showing that stimulation of D_5R, not D_1R, leads to the degradation of AT_1R in RPTCs, which could be completely blocked by clasto-lactacystin beta-lactone, a proteasome inhibitor [46]. Studies have shown that SNXs are involved in the protein degradation, for example, SNX1 has been suggested to sort protease-activated receptor-1 from early endosomes to lysosomes for its degradation [66]. In our study, the proteasomal inhibition, rather than lysosomal inhibition, increased AT_1R expression in A10 cells, and the increment was more pronounced after siSNX1 knockdown, accompanied by decreased interaction between ubiquitin and AT_1R. We also found that AT_1R was mainly colocalized with PSMD6, a proteasomal marker, rather than LAMP1, a lysosomal marker, at the cytoplasm of A10 cells, and the colocalization of AT_1R and PSMD6 was decayed after SNX1 knockdown. These indicate that SNX1-mediated AT_1R degradation is mainly through the proteasomal pathway, not the lysosomal pathway.

In conclusion, our data reveal a crucial role of SNX1 in AT_1R sorting and degradation in VSMCs. Depletion of SNX1 results in higher AT_1R mediated-mesenteric artery contractility, which may represent a novel mechanism for the regulation of blood pressure.

Supplementary Material

Refer to Web version on PubMed Central for supplementary material.

Acknowledgements

These studies were supported, in part, by grants from the National Natural Science Foundation of China (31730043, 81570379), National Key R&D Program of China (2018YFC1312700), Program of Innovative Research Team by National Natural Science Foundation (81721001), Program for Changjiang Scholars and Innovative Research Team in University (IRT1216), grant from The Third Affiliated Hospital of Chongqing Medical University (KY19024), and National Institutes of Health (R01-DK039308, P01-HL074940).

References

1. Zhou B, Danaei G Stevens GA, Bixby H, Taddei C, Carrillo-Larco RM, et al. Long-term and recent trends in hypertension awareness, treatment, and control in 12 high-income countries: an analysis of 123 nationally representative surveys. The Lancet. 2019;394(10199):639–651.
2. Ettehad D, Emdin CA, Kiran A, Anderson SG, Callender T, Emberson J, et al. Blood pressure lowering for prevention of cardiovascular disease and death: a systematic review and meta-analysis. The Lancet. 2016;387(10022):957–967.
3. Forouzanfar MH, Liu P, Roth GA, Ng M, Biryukov S, Marczak L, et al. Global burden of hypertension and systolic blood pressure of at least 110 to 115 mm Hg, 1990-2015. JAMA. 2017;317(2): 165–182. [PubMed: 28097354]
4. Bohr DF, Dominiczak A, Webb RC. Pathophysiology of the vasculature in hypertension. Hypertension. 1991;18(5_supplement):III69. [PubMed: 1937688]
5. Brown IAM, Diederich L, Good ME, DeLalio LJ, Murphy SA, Cortese-Krott MM, et al. Vascular Smooth Muscle Remodeling in Conductive and Resistance Arteries in Hypertension. Arterioscler Thromb Vasc Biol. 2018;38(9):1969–1985. [PubMed: 30354262]
6. Laurent S, Boutouyrie P. The structural factor of hypertension: large and small artery alterations. Circ Res. 2015;116(6):1007–1021. [PubMed: 25767286]
7. Chen K, Fu C, Chen C, Liu L, Ren H, Han Y, et al. Role of GRK4 in the regulation of arterial AT1 receptor in hypertension. Hypertension. 2014;63(2):289–296. [PubMed: 24218433]
8. Wang Z, Zeng C, Villar VAM, Chen S-Y, Konkalmatt P, Wang X, et al. Human GRK4γ 142V Variant Promotes Angiotensin II Type I Receptor–Mediated Hypertension via Renal Histone Deacetylase Type 1 Inhibition. Hypertension. 2016;67(2):325–334. [PubMed: 26667412]
9. Wynne BM, Chiao C-W, Webb RC. Vascular smooth muscle cell signaling mechanisms for contraction to angiotensin II and endothelin-1. J Am Soc Hypertens. 2009;3(2):84–95. [PubMed: 20161229]
10. Nickenig G, Harrison DG. The AT1-type angiotensin receptor in oxidative stress and atherogenesis: part I: oxidative stress and atherogenesis. Circulation. 2002;105(3):393–396. [PubMed: 11804998]
11. Vaziri ND, Bai Y, Ni Z, Quiroz Y, Pandian R, Rodriguez-Iturbe B. Intra-renal angiotensin II/AT1 receptor, oxidative stress, inflammation, and progressive injury in renal mass reduction. J Pharmacol Exp Ther. 2007;323(1):85–93. [PubMed: 17636006]
12. Sanz-Rosa D, Oubina MP, Cediel E, de las Heras N, Vegazo O, Jiménez J, et al. Effect of AT1 receptor antagonism on vascular and circulating inflammatory mediators in SHR: role of NF-κB/IκB system. American Journal of Physiology-Heart and Circulatory Physiology. 2005;288(1):H111–H115. [PubMed: 15308481]
13. Smith GR, Missailidis S. Cancer, inflammation and the AT1 and AT2 receptors. J Inflamm. 2004;1(1):3.
14. Williams B. Angiotensin II and the pathophysiology of cardiovascular remodeling. The American journal of cardiology. 2001;87(8):10–17.
15. Takemoto M, Egashira K, Tomita H, Usui M, Okamoto H, Kitabatake A, et al. Chronic angiotensin-converting enzyme inhibition and angiotensin II type 1 receptor blockade: effects on cardiovascular remodeling in rats induced by the long-term blockade of nitric oxide synthesis. Hypertension. 1997;30(6):1621–1627. [PubMed: 9403592]
16. Yang J, Van Anthony MV, Rozyyev S, Jose PA, Zeng C. The emerging role of sorting nexins in cardiovascular diseases. Clin Sci. 2019;133(5):723–737.
17. Zhang H, Huang T, Hong Y, Yang W, Zhang X, Luo H, et al. The retromer complex and sorting nexins in neurodegenerative diseases. Frontiers in aging neuroscience. 2018;10:79. [PubMed: 29632483]
18. Teasdale RD, Collins BM. Insights into the PX (phox-homology) domain and SNX (sorting nexin) protein families: structures, functions and roles in disease. Biochem J. 2012;441(1):39–59. [PubMed: 22168438]
19. Worby CA, Dixon JE. Sorting out the cellular functions of sorting nexins. Nat Rev Mol Cell Biol. 2002;3(12):919. [PubMed: 12461558]

20. Van Anthony MV, Jones JE, Armando I, Asico LD, Escano CS, Lee H, et al. Sorting nexin 1 loss results in D5 dopamine receptor dysfunction in human renal proximal tubule cells and hypertension in mice. J Biol Chem. 2013;288(1):152–163. [PubMed: 23152498]
21. Villar VAM, Armando I, Sanada H, Frazer LC, Russo CM, Notario PM, et al. Novel role of sorting nexin 5 in renal D1 dopamine receptor trafficking and function: implications for hypertension. The FASEB Journal. 2013;27(5):1808–1819. [PubMed: 23195037]
22. Li F, Yang J, Jones JE, Villar VAM, Yu P, Armando I, et al. Sorting nexin 5 and dopamine D1 receptor regulate the expression of the insulin receptor in human renal proximal tubule cells. Endocrinology. 2015;156(6):2211–2221. [PubMed: 25825816]
23. Drake MT, Shenoy SK, Lefkowitz RJ. Trafficking of G protein–coupled receptors. Circ Res. 2006;99(6):570–582. [PubMed: 16973913]
24. Carlton J, Bujny M, Peter BJ, Oorschot VM, Rutherford A, Mellor H, et al. Sorting nexin-1 mediates tubular endosome-to-TGN transport through coincidence sensing of high-curvature membranes and 3-phosphoinositides. Curr Biol. 2004;14(20):1791–1800. [PubMed: 15498486]
25. Zeng C, Jose PA. Dopamine receptors: important antihypertensive counterbalance against hypertensive factors. Hypertension. 2011;57(1):11–17. [PubMed: 21098313]
26. Gildea JJ. Dopamine and angiotensin as renal counter regulatory systems controlling sodium balance. Curr Opin Nephrol Hypertens. 2009;18(1):28. [PubMed: 19077686]
27. Wang Y, Thatcher SE, Cassis LA. Measuring blood pressure using a noninvasive tail cuff method in mice. In: The Renin-Angiotensin-Aldosterone System.) Springer2017, 69–73.
28. Lin P, Wu M, Qin J, Yang J, Ye C, Wang C. Magnesium lithospermate B improves renal hemodynamics and reduces renal oxygen consumption in 5/6th renal ablation/infarction rats. BMC Nephrol. 2019;20(1):49. [PubMed: 30755161]
29. Cheng Z, Zhang M, Hu J, Lin J, Feng X, Wang S, et al. Cardiac - specific Mst1 deficiency inhibits ROS - mediated JNK signalling to alleviate Ang II - induced cardiomyocyte apoptosis. J Cell Mol Med. 2019;23(1):543–555. [PubMed: 30338935]
30. Mulvany MJ, Halpern W. Contractile properties of small arterial resistance vessels in spontaneously hypertensive and normotensive rats. Circ Res. 1977;41(1):19–26. [PubMed: 862138]
31. Yao Y, Wang W, Li M, Ren H, Chen C, Wang J, et al. Curcumin exerts its anti-hypertensive effect by down-regulating the AT 1 receptor in vascular smooth muscle cells. Scientific reports. 2016;6:25579. [PubMed: 27146402]
32. Fu J, Han Y, Wang J, Liu Y, Zheng S, Zhou L, et al. Irisin lowers blood pressure by improvement of endothelial dysfunction via AMPK - Akt - eNOS - NO pathway in the spontaneously hypertensive Rat. Journal of the American Heart Association. 2016;5(11):e003433. [PubMed: 27912206]
33. Fu J, Han Y, Wang H, Wang Z, Liu Y, Chen X, et al. Impaired dopamine D 1 receptor-mediated vasorelaxation of mesenteric arteries in obese Zucker rats. Cardiovasc Diabetol. 2014;13(1):50. [PubMed: 24559270]
34. Wu LP, Gong ZF, Wang H, Zhou ZS, Zhang MM, Liu C, et al. TSPO ligands prevent the proliferation of vascular smooth muscle cells and attenuate neointima formation through AMPK activation. Acta Pharmacol Sin. 2020;41(1):34–46. [PubMed: 31515530]
35. Xu H, Zhang H, Liu G, Kong L, Zhu X, Tian X, et al. Coumarin-Based Fluorescent Probes for Super-resolution and Dynamic Tracking of Lipid Droplets. Anal Chem. 2019;91(1):977–982. [PubMed: 30507133]
36. Bigarella CL, Borges L, Costa FF, Saad ST. ARHGAP21 modulates FAK activity and impairs glioblastoma cell migration. Biochim Biophys Acta. 2009; 1793(5):806–816. [PubMed: 19268501]
37. Han JM, Jeong SJ, Park MC, Kim G Kwon NH, Kim HK, et al. Leucyl-tRNA synthetase is an intracellular leucine sensor for the mTORC1-signaling pathway. Cell. 2012; 149(2):410–424. [PubMed: 22424946]
38. Liu C, Hu YH, Han Y, Wang YB, Zhang Y, Zhang XQ, et al. MG53 protects against contrast-induced acute kidney injury by reducing cell membrane damage and apoptosis. Acta Pharmacol Sin. 2020(e-pub ahead of print 2020/05/20; doi:10.1038/s41401-020-0420-8).

39. Liu C, Chen K, Wang H, Zhang Y, Duan X, Wang H, et al. Gastrin Attenuates Renal Ischemia/Reperfusion Injury by a PI3K/Akt/Bad-Mediated Anti-apoptosis Signaling. Frontiers in Pharmacology. 2020;11:1672.
40. Gavet O, Pines J. Progressive activation of CyclinB1-Cdk1 coordinates entry to mitosis. Dev Cell. 2010;18(4):533–543. [PubMed: 20412769]
41. Jin SW, Choi CY, Hwang YP, Kim HG, Kim SJ, Chung YC, et al. Betulinic acid increases eNOS phosphorylation and no synthesis via the calcium-signaling pathway. J Agric Food Chem. 2016;64(4):785–791. [PubMed: 26750873]
42. Li H, Armando I, Yu P, Escano C, Mueller SC, Asico L, et al. Dopamine 5 receptor mediates Ang II type 1 receptor degradation via a ubiquitin-proteasome pathway in mice and human cells. The Journal of clinical investigation. 2008;118(6):2180–2189. [PubMed: 18464932]
43. Do KH, Kim MS, Kim JH, Rhim B-Y, Lee WS, Kim CD, et al. Angiotensin II-induced aortic ring constriction is mediated by phosphatidylinositol 3-kinase/L-type calcium channel signaling pathway. Exp Mol Med. 2009;41(8):569. [PubMed: 19381068]
44. Wang X, Zhao Y, Zhang X, Badie H, Zhou Y, Mu Y, et al. Loss of sorting nexin 27 contributes to excitatory synaptic dysfunction by modulating glutamate receptor recycling in Down's syndrome. Nat Med. 2013;19(4):473. [PubMed: 23524343]
45. Mangieri LR, Mader BJ, Thomas CE, Taylor CA, Luker AM, Tse TE, et al. ATP6V0C knockdown in neuroblastoma cells alters autophagy-lysosome pathway function and metabolism of proteins that accumulate in neurodegenerative disease. PLoS ONE. 2014;9(4):e93257. [PubMed: 24695574]
46. Gildea JJ, Wang X, Jose PA, Felder RA. Differential D1 and D5 receptor regulation and degradation of the angiotensin type 1 receptor. Hypertension. 2008;51(2):360–366. [PubMed: 18172057]
47. Kurten RC, Cadena DL, Gill GN. Enhanced degradation of EGF receptors by a sorting nexin, SNX1. Science. 1996;272(5264):1008–1010. [PubMed: 8638121]
48. Kurten RC, Eddington AD, Chowdhury P, Smith RD, Davidson AD, Shank BB. Self-assembly and binding of a sorting nexin to sorting endosomes. J Cell Sci. 2001;114(9):1743–1756. [PubMed: 11309204]
49. Yang J, Asico LD, Beitelshees AL, Feranil JB, Wang X, Jones JE, et al. Sorting nexin 1 loss results in increased oxidative stress and hypertension. FASEB J. 2020(e-pub ahead of print 2020/04/16;doi:10.1096/fj.201902448R).
50. Wilde E, Aubdool AA, Thakore P, Baldissera L Jr., Alawi KM, Keeble J, et al. Tail-Cuff Technique and Its Influence on Central Blood Pressure in the Mouse. J Am Heart Assoc. 2017;6(6).
51. Arun K, Kaul C, Ramarao P. High glucose concentration augments angiotensin II mediated contraction via AT1 receptors in rat thoracic aorta. Pharmacol Res. 2004;50(6):561–568. [PubMed: 15501693]
52. Navar LG, Harrison-Bernard LM, Imig JD, Wang C-T, Cervenka L, Mitchell KD. Intrarenal angiotensin II generation and renal effects of AT1 receptor blockade. Journal of the American Society of Nephrology: JASN. 1999;10:S266–272. [PubMed: 10201881]
53. Qadri F, Culman J, Veltmar A, Maas K, Rascher W, Unger T. Angiotensin II-induced vasopressin release is mediated through alpha-1 adrenoceptors and angiotensin II AT1 receptors in the supraoptic nucleus. J Pharmacol Exp Ther. 1993;267(2):567–574. [PubMed: 8246129]
54. Zheng H, Li Y-F, Wang W, Patel KP. Enhanced angiotensin-mediated excitation of renal sympathetic nerve activity within the paraventricular nucleus of anesthetized rats with heart failure. American Journal of Physiology-Regulatory, Integrative and Comparative Physiology. 2009;297(5):R1364–R1374.
55. Zhang Z, Li M, Lu R, Alioua A, Stefani E, Toro L. The angiotensin II type 1 receptor (AT_1R) closely interacts with large conductance voltage- and Ca2+-activated K+ (BK) channels and inhibits their activity independent of G-protein activation. J Biol Chem. 2014;289(37):25678–25689. [PubMed: 25070892]
56. Do KH, Kim MS, Kim JH, Rhim BY, Lee WS, Kim CD, et al. Angiotensin II-induced aortic ring constriction is mediated by phosphatidylinositol 3-kinase/L-type calcium channel signaling pathway. Exp Mol Med. 2009;41(8):569–576. [PubMed: 19381068]

57. Kao SH, Wang WL, Chen CY, Chang YL, Wu YY, Wang YT, et al. Analysis of Protein Stability by the Cycloheximide Chase Assay. Bio Protoc. 2015;5(1).
58. Buchanan BW, Lloyd ME, Engle SM, Rubenstein EM. Cycloheximide Chase Analysis of Protein Degradation in Saccharomyces cerevisiae. J Vis Exp. 2016(e-pub ahead of print 2016/05/12;doi:10.3791/53975)(110).
59. Comeau JW, Costantino S, Wiseman PW. A guide to accurate fluorescence microscopy colocalization measurements. Biophys J. 2006;91(12):4611–4622. [PubMed: 17012312]
60. Shulei W, Arena ET, Eliceiri KW, Ming Y. Automated and Robust Quantification of Colocalization in Dual-Color Fluorescence Microscopy: A Nonparametric Statistical Approach. IEEE Trans Image Process. 2018;27(2):622–636. [PubMed: 29053465]
61. Bolte S, Cordelières FP. A guided tour into subcellular colocalization analysis in light microscopy. J Microsc. 2006;224(Pt 3):213–232. [PubMed: 17210054]
62. Wang X, Robbins J. Proteasomal and lysosomal protein degradation and heart disease. J Mol Cell Cardiol. 2014;71:16–24. [PubMed: 24239609]
63. Ciechanover A. The ubiquitin-proteasome proteolytic pathway. Cell. 1994;79(1):13–21. [PubMed: 7923371]
64. Hanyaloglu AC, Zastrow Mv. Regulation of GPCRs by endocytic membrane trafficking and its potential implications. Annu Rev Pharmacol Toxicol. 2008;48:537–568. [PubMed: 18184106]
65. Wojcikiewicz RJ. Regulated ubiquitination of proteins in GPCR-initiated signaling pathways. Trends Pharmacol Sci. 2004;25(1):35–41. [PubMed: 14723977]
66. Wang Y, Zhou Y, Szabo K, Haft CR, Trejo J. Down-regulation of protease-activated receptor-1 is regulated by sorting nexin 1. Mol Biol Cell. 2002;13(6):1965–1976. [PubMed: 12058063]

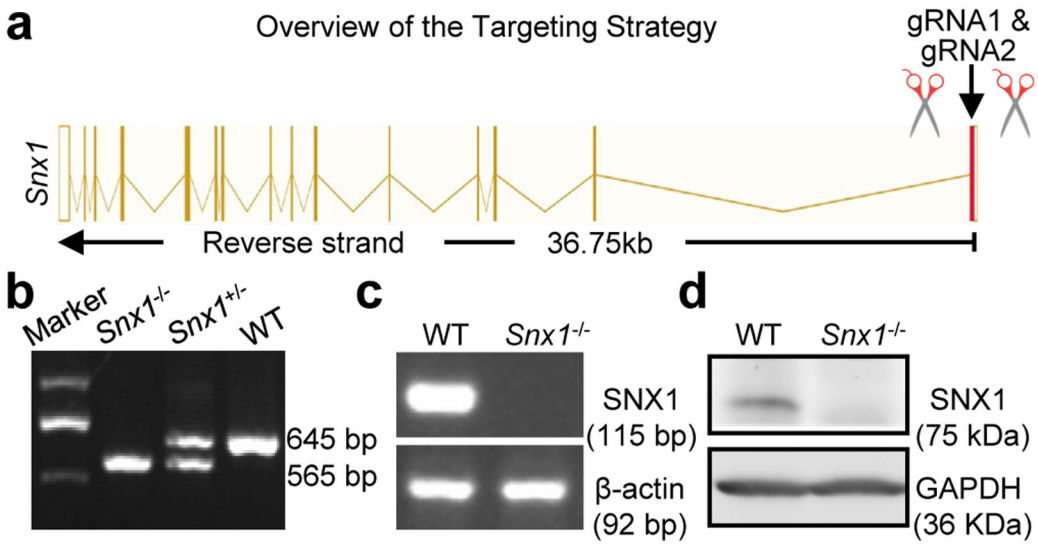

Fig. 1. Generation and identification of *Snx1*$^{-/-}$ mice.

a Schematic diagram showing the generation of *Snx1*$^{-/-}$ mice based on CRISPR/Cas9. **b** Agarose gel electrophoresis demonstrating genotype determinations using DNA from three individuals representing *Snx1*$^{-/-}$, *Snx1*$^{+/-}$, and WT mice. **c** Representative images of the agarose gel electrophoresis of qPCR products, indicating the expression of SNX1 mRNA in aortas from WT mice, but not from *Snx1*$^{-/-}$ mice. **d** Immunoblots showing the expression of SNX1 protein in aortas from WT mice, but not from *Snx1*$^{-/-}$ mice.

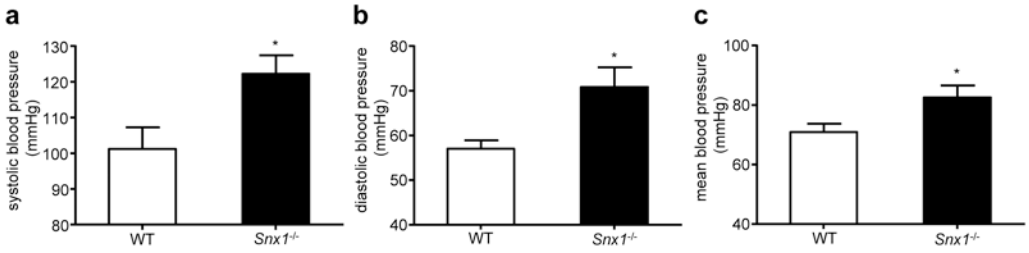

Fig. 2. Elevated blood pressure in *Snx1*$^{-/-}$ mice measured using the tail-cuff plethysmography.

a The systolic blood pressure was increased in *Snx1*$^{-/-}$ mice compared to wild-type (WT) littermates (122.0 ± 4.2 mm Hg *vs.* 99.8 ± 3.3 mm Hg, **P*<0.05 vs. WT, *n*=5). **b** Increased diastolic blood pressure in *Snx1*$^{-/-}$ mice compared to WT littermates (69.6 ± 2.8 mm Hg *vs.* 59.4 ± 3.1 mm Hg, **P*<0.05 vs. WT, *n*=5). **c** Elevated mean blood pressure in *Snx1*$^{-/-}$ mice compared to WT littermates (80.8 ± 3.1 mm Hg *vs.* 67.8 ± 2.2 mm Hg, **P*<0.05 vs. WT, *n*=5).

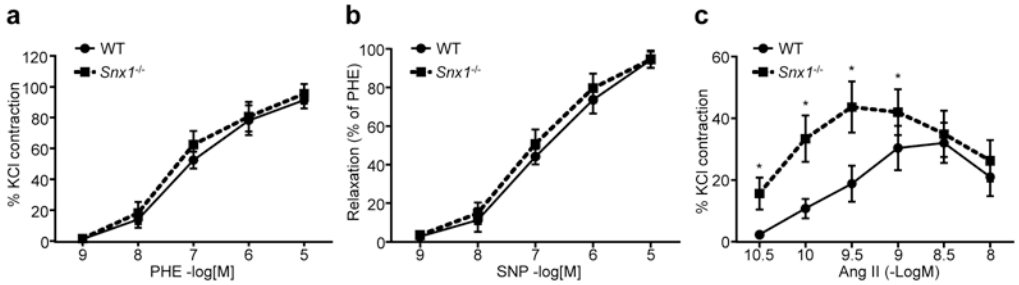

Fig. 3. Enhanced reactivity of mesenteric artery to Ang II in *Snx1*$^{-/-}$ mice.

a Phenylephrine (PHE)-induced contractions of mouse mesenteric arteries were not changed in *Snx1*$^{-/-}$ mice, no significant difference between WT and *Snx1*$^{-/-}$ mice (n=5). **b** Sodium nitroprusside (SNP)-induced relaxations of mouse mesenteric arteries were not remarkable changed in *Snx1*$^{-/-}$ mice (n=5). **c** Ang II-induced contractions of mouse mesenteric arteries were increased in *Snx1*$^{-/-}$ mice (*P<0.05 vs. WT, n=5).

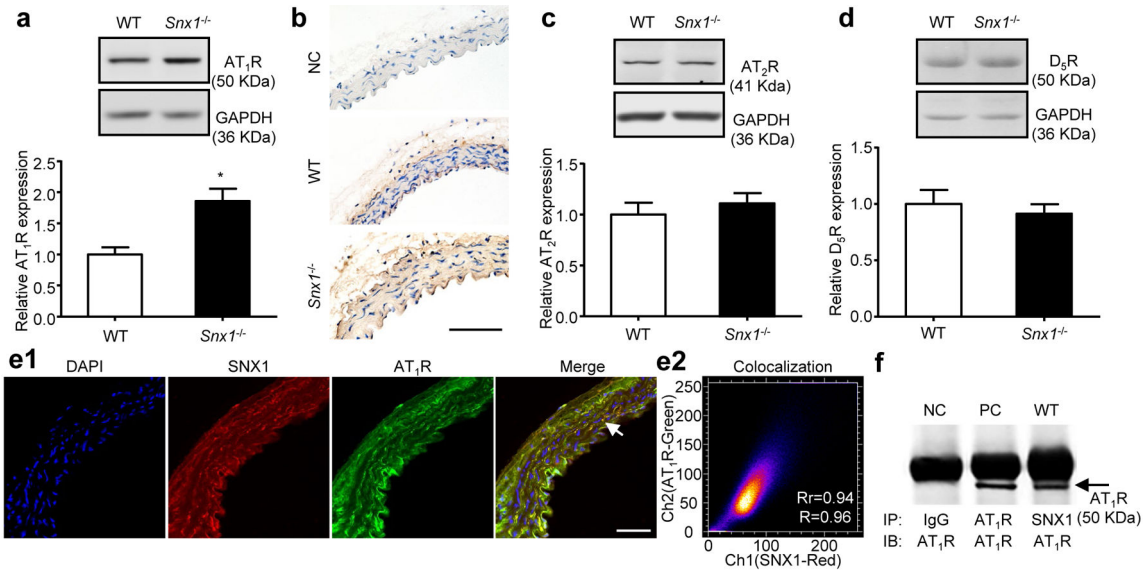

Fig. 4. Increased AT_1R expression in aortas from *Snx1*$^{-/-}$ mice.

a AT_1R protein level was upregulated in the aortas from *Snx1*$^{-/-}$ mice (**P*<0.05 vs. WT, *n*=5). **b** Immunohistochemistry staining of AT_1R revealed increased expression of AT_1R in *Snx1*$^{-/-}$ mice compared to WT mice (these studies were repeated 3 times; NC, negative control; scale bar = 50 μm). **c** AT_2R expression was not changed in the aortas from *Snx1*$^{-/-}$ mice, analyzed by immunoblotting (*n*=5). **d** D_5R expression was not changed in the aortas from *Snx1*$^{-/-}$ mice, analyzed by immunoblotting (*n*=3). **e** The colocalization of AT_1R and SNX1 detected by immunofluorescence laser confocal microscopy. Representative images suggesting the colocalization of AT_1R and SNX1 in aortic sections from WT mice (scale bar = 50 μm) (**e1**). The quantification of colocalization was analyzed by ImageJ Colocalization Finder plugin, and the Pearson's correlation coefficient (Rr) and the overlap coefficient (R) were calculated (**e2**). **f** Immunoprecipitation assay indicated the interaction between AT_1R and SNX1 in the aortas from WT mice (these studies were repeated 3 times; NC, negative control; PC, positive control).

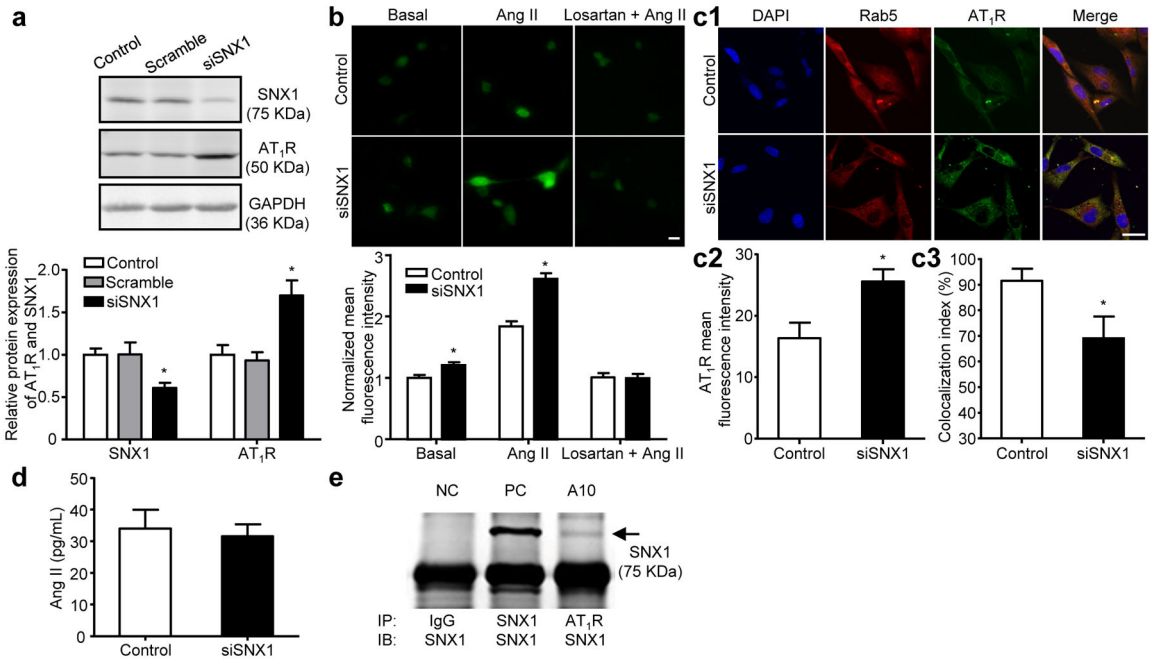

Fig. 5. Upregulated AT_1R protein level in SNX1 knockdown A10 cells.

a AT_1R protein level was upregulated after SNX1 knockdown, indicated by immunoblotting studies (**P*<0.05 vs. control, *n*=3). **b** Intracellular calcium concentration was increased in SNX1 knockdown A10 cells, revealed by representative images of Fluo-4 AM fluorescent (**b1**) and the statistic results (**b2**) (scale bar = 20 μm, **P*<0.05 vs. control, *n*=3). **c** The colocalization of AT_1R and Rab5 detected by immunofluorescence laser confocal microscopy. Representative images revealing the colocalization of AT_1R and Rab5 in control and siSNX1-treated A10 cells (scale bar = 20 μm) (**c1**). AT_1R mean fluorescence intensity was quantified by ImageJ (**P*<0.05 vs. control, *n*=10 cells) (**c2**). The quantification of colocalization was analyzed by ImageJ Colocalization Finder plugin, the index of colocalization corresponds to the mean ± standard deviation (SD) of the overlap coefficient (R)×100 (**P*<0.05 vs. control, *n*=10 cells) (**c3**). **d** Ang II concentration in the supernatant of cultured A10 cells was not changed after SNX1 knockdown, determined by enzyme-linked immunosorbent assay (ELISA) (*n*=3). **e** Immunoprecipitation analysis of the interaction between SNX1 and AT_1R in A10 cells (these studies were repeated 3 times; NC, negative control; PC, positive control).

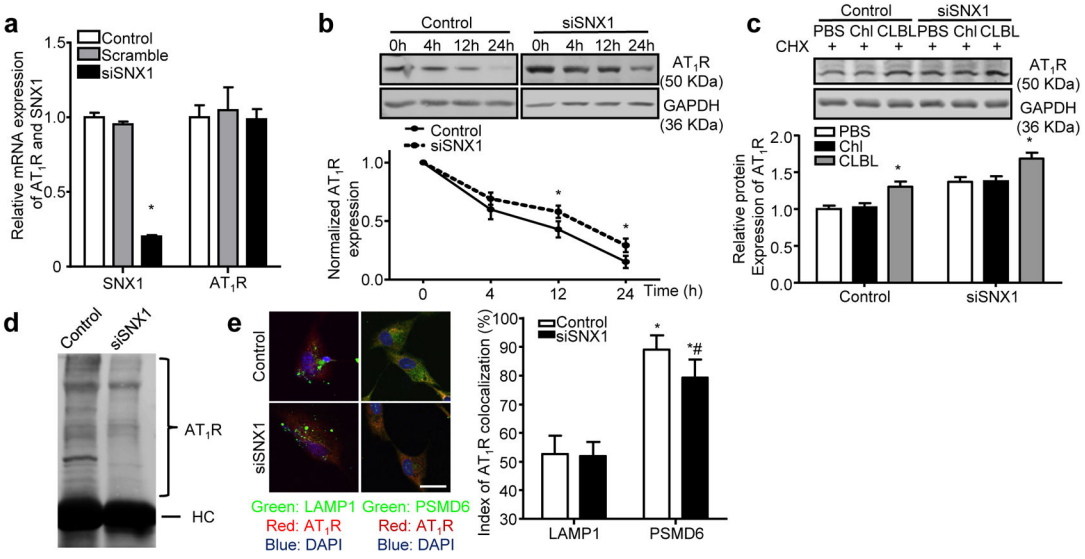

Fig. 6. Involvement of the proteasome pathway in SNX1-mediated AT_1R protein degradation.

a The AT_1R mRNA level, determined by qPCR, was not changed after SNX1 knockdown (**P*<0.05 vs. control, *n*=3). **b** The degradation of AT_1R protein was reduced when SNX1 knockdown, as reflected by immunoblotting. The cells were incubated with cycloheximide (500 μmol/L) for indicated times. Results are expressed as the percentage change of the control in each group (**P*<0.05 vs. *n*=3). **c** Proteasome but not lysosome inhibition increased AT_1R protein expression, and the increment was more pronounced in siSNX1-treated A10 cells. (500 μmol/L cycloheximide was co-administered; CHX, cycloheximide; Chl: chloroquine, a lysosomal inhibitor, 100 μmol/L; CLBL: clasto-lactacystin beta-lactone, a proteasomal inhibitor, 10 μmol/L, **P*<0.05 vs. control, *n*=3). **d** Immunoprecipitation analysis indicates a decayed interaction between AT_1R and ubiquitin when SNX1 knockdown. **e** Representative images of immunofluorescence laser confocal microscopy and the quantification of colocalization indicated that AT_1R mainly colocalized with PSMD6 (a proteasomal marker) rather than LAMP1 (a lysosomal marker), and the colocalization of AT_1R and PSMD6 was reduced after SNX1 knockdown. The quantification of colocalization was analyzed by ImageJ Colocalization Finder plugin, the index of colocalization corresponds to the mean ± standard deviation (SD) of the overlap coefficient (R) ×100 (scale bar = 20 μm, **P*<0.05 vs. control, *n*=10 cells).

Table 1

Primers sequences used for qPCR

Gene Name	Gene Bank Number	Primer Sequence (5'-3')	Product Size (bp)
Mouse SNX1	NM_019727.2	Foreword: ATGGATCCGGAGTCGGAAGGG Reverse: GAGACTGGGGCTTAGTGGCTG	115
Mouse β-actin	NM_007393.5	Foreword: TAAAACCCGGCGGCGCAA Reverse: GGTGTGGACCGGCAACGAA	92
Rat SNX1	NM_053411.1	Foreword: CGACTCCCTCCGCCCTTC Reverse: ACTGGGGCTTACTAGCTGCC	136
Rat AT_1R	NM_030985.4 NM_031009.2	Foreword: AGCATCATCTTTGTGGTGGGAA Reverse: AAGTAAATGACAATCACCACCAAGC	59
Rat GAPDH	NM_017008.4	Foreword: AACACGGAAGGCCATGCCAG Reverse: GCATCCACTGGTGCTGCCAA	81